

S.R. Deshiikan
K.D. Papadopoulos

Visual microscopic studies on hetero-aggregation and selective aggregation

Received: 4 July 1996
Accepted: 5 December 1996

Abstract An optical video microscopic technique was used to study hetero-aggregation and selective aggregation phenomena among *n*-hexadecane oil drops (40–110 μm in diameter) and two types of polystyrene latex particles (6.76 and 30.2 μm , in diameter), suspended inside an aqueous medium with pH varying between 1.1 and 12.9. A single drop was produced in situ using a micropipette inside the aqueous phase-filled glass microcapillary (100–160 μm i.d.) containing the particles. Interactions between the drop and the solid particles and among the solid particles was achieved by movement of the aqueous medium in and out of a second micropipette. Drop-particle interactions were distinctly different from particle-particle interactions. It was observed that the latex particles aggregated irreversibly with the oil drop in all cases except two, viz. for 6.76 μm particles at around neutral pH whereas the irreversibility of aggregation in particle-particle interactions was only seen at the

ends of the pH spectrum. At around neutral pH, the flocs or clusters of small particles were very weak. Visual observations at each pH are explained on the basis of the classical DLVO (Derjaguin–Landau–Verwey–Overbeek) theory. Partial wetting of particles surfaces by oil appears to be a key factor in the irreversibility of drop-particle hetero-aggregation. Results indicate that the display of reversible, irreversible or weak aggregation depends on the location and depth of the secondary minimum and that the long-range, attractive, London–van der Waals force is responsible for the initial formation of an aggregate.

Key words Optical video microscopy – polystyrene latex particles – hexadecane oil drops – aggregation – flocculation – coagulation – hetero – homo – selective – partial wetting – zeta potential – Debye length – total interaction free energy – DLVO theory – London–van der Waals – electrical double layer – secondary minimum

Dr. S.R. Deshiikan
Prof. Dr. K.D. Papadopoulos (✉)
Suite 300, Lindy Boggs Building
Department of Chemical Engineering
Tulane University
New Orleans, Louisiana 70118, USA

Introduction

Hetero-aggregation and selective aggregation among oil drops and particles is of practical importance in many natural and industrial systems. For example, both phe-

nomena are fundamental to selectivity and efficiency in separation processes such as flotation, desliming, coagulation, flocculation, decoloring, etc., used in the ceramic and mineral industry [1–6]. In the beneficiation of ores by oil-flotation, the first step is the attachment of the finely divided particles on the surfaces of oil droplets produced in

the suspension. The extent of attachment of the mineral particle to the drop depends upon the surface-to-surface interactions between the mineral and the oil drop. Once the mineral is separated from the suspension and is concentrated with the oil, conditions are altered to promote coalescence of the drops and achieve selective aggregation between the particles. In this final stage of separation, wetting and spreading of oil on mineral surfaces can become very important. Besides mineral suspensions, mixtures of oil drops and solid particles are also found in formulations of paints, inks, cosmetics, pharmaceutical and drug suspensions, agricultural dispersions, coating products and food emulsions [2]. Also, environmental remediation processes for waste volume reduction and recycling depend on hetero-aggregation and selective aggregation since waste waters most frequently contain solid as well as liquid dispersed matter [7]. In all the above situations, it is crucial to understand the drop-drop, drop-particle and particle-particle interactions at the microscopic level. Published theories [3–6, 8–10] describe the kinetics of such processes in bulk, whereas there are no reports on actual visualization of hetero-aggregation or selective aggregation in systems containing oil drops and solid particles.

In recent years an optical video-microscopy technique has been developed and used in our laboratory for studying: the effects of colloidal forces on the coalescence of microscopic oil drops [11, 12], the random motility and chemotaxis of bacteria in capillaries [13, 14], the electrokinetic transport of settled spherical particles in capillaries of comparable diameters [15], and the stability of water-in-oil-in-water vesicular globules [16]. In this paper we report visual observations of hetero-aggregation and selective aggregation phenomena among oil drops and polystyrene latex particles of two different sizes (6.76 and 30.2 μm , diameter) as the solution pH was varied from 1.1 to 12.9. No surfactants or neutral salts were employed. The results are explained in terms of the classical DLVO (Derjaguin–Landau–Verwey–Overbeek) interactions which form the basis of many hetero-aggregation and selective-aggregation theories.

An analysis of the aggregation process and the DLVO theory

In a suspension containing particles and drops, the first step in the formation of an aggregate is the mutual approach of the surfaces of two particles, two droplets, or a droplet and a particle toward each other. This process can be initiated by Brownian motion, gravity, fluid forces or other external forces. Once the surfaces come in close proximity of each other (typically at surface separations less than 300 nm) the intervening fluid can be treated as

a thin film. Fluid drains from the thin film at a rate dictated by hydrodynamic as well as surface forces. In the coalescence of drops, it has been shown [17] that the surface interaction forces become significant when the intervening film has drained to a thickness of about 100 nm and can become the deciding factors in coalescence, hetero-aggregation and selective aggregation of microscopic drops and particles [2]. Surface interaction forces are fundamental to theories and models [3–6, 8–10] describing the kinetics of aggregation processes. The visible effects of these forces were clearly demonstrated in previous studies [11, 12] on the coalescence of microscopic oil drops.

The predominant and better understood surface forces are those due to the London-van der Waals (LvdW) and the electrostatic double layer (EDL) interactions, which form the basis of the classical DLVO theory [18, 19], developed to predict the stability of colloid suspensions against aggregation. Other surface forces that were not included in the original formalism of the DLVO theory, but have now been recognized to also affect the stability of colloidal dispersions under special conditions, are the solvation or hydration forces, the hydrophobic forces, the depletion forces, and steric forces [2]. Hydration or solvation forces are important only at very close separations (generally smaller than 5 nm) and the effect of the other non-DLVO forces is negligible in the absence of surfactants, polymers or other impurities [2].

For two spheres of radii a_1 and a_2 , made of material α and β , respectively, and interacting in a third medium, γ , the LvdW interaction free energy (V_H) at a surface separation distance h is given by the well known Hamaker expression [2]:

$$V_H(h) = -\frac{A_{\alpha\gamma\beta}}{6h} \left[\frac{a_1 a_2}{a_1 + a_2} \right]. \quad (1)$$

In the above equation $A_{\alpha\gamma\beta}$ is the Hamaker constant and depends on material properties of the spheres and the intervening medium. The Hamaker constant for the polystyrene latex–water–polystyrene latex system is 9.5×10^{-21} J [2]. For the *n*-hexadecane–water–polystyrene latex system the Hamaker constant is 7.16×10^{-21} J which is obtained as the geometric mean of the Hamaker constants for the oil–water–oil system and polystyrene–water–polystyrene system [2].

The EDL interaction free energy (V_R), expressed in Joules, for two dissimilar spheres was described in a recent paper by Sader et al. [20] as a modification of the original Hogg–Healey–Fuersteneau (HHF) formula [6]:

$$V_R(h) = \frac{\varepsilon}{4} \left(\frac{a_1 a_2}{a_1 + a_2 + h} \right) [(\psi_1 + \psi_2)^2 \ln(1 + e^{-\kappa h}) + (\psi_1 - \psi_2)^2 \ln(1 - e^{-\kappa h})], \quad (2)$$

where ε is the dielectric permittivity of the medium, ψ_1 and ψ_2 are the surface potentials of the spheres with radii a_1 and a_2 , and κ the Debye parameter. While this equation is generally applicable for low surface potentials, Sader et al. [20] have also provided the following expression for V_R at high surface potentials:

$$V_R(h) = \varepsilon \left[\frac{kT}{e_0} \right]^2 Y^2(h) \left(\frac{a^2}{2a+h} \right) \ln [1 + e^{-\kappa h}], \quad (3)$$

where

$$Y(h) = 4e^{\kappa h/2} \tanh^{-1} \left[e^{-\kappa h/2} \tanh \left(\frac{y_s}{4} \right) \right]. \quad (4)$$

In the above expression, y_s is the dimensionless surface potential (normalized with kT/e_0), k is the Boltzmann constant and e_0 the electronic charge. In this paper, the surface potentials of the polystyrene spheres and oil drops are assumed to be represented by their zeta potentials and Eqs. (2) and (3) are used to compute the EDL interaction free energy. The London–van der Waals interaction free energy is computed through Eq. (1), which ignores retardation effects.

The experiments

The surfactant-free 6.76 μm diameter polystyrene latex particles (sulfate type) were supplied by Interfacial Dynamics Corp., Portland, OR, and the 30.2 μm diameter polystyrene particles (Dynospheres) were obtained from Japan Synthetic Rubber, Japan. The particles were dispersed in dilute solutions of HCl and NaOH of known pH. Doubly deionized, filtered and singly distilled E-PureTM water was used to make the solutions. HCl and NaOH were obtained from Aldrich Chemical Co., WI, and had purity exceeding 99.99%. The electrophoretic mobilities of the large particles were measured at varying pH using a model MK II microelectrophoresis apparatus, supplied by Rank Brothers Ltd., Cambridge, England, capable of measuring the electrophoretic mobility of large settling particles. To convert the mobility data to zeta potentials, an accurate estimate of the ionic strength was required. For this, it was necessary to measure the background electrolyte concentration in the stock dispersions supplied by the particle manufacturers. Atomic absorption data on the supernatant phase of both dispersions showed the presence of sodium. Assuming Na^+ to be the only cation apart from H^+ , the concentration of sodium ions in the stock dispersion was estimated from measurements of pH and conductivity of the aqueous solution, with and without the addition of a fixed quantity of the stock dispersion. Once the concentrations of all the ions (H^+ , Na^+ , OH^-

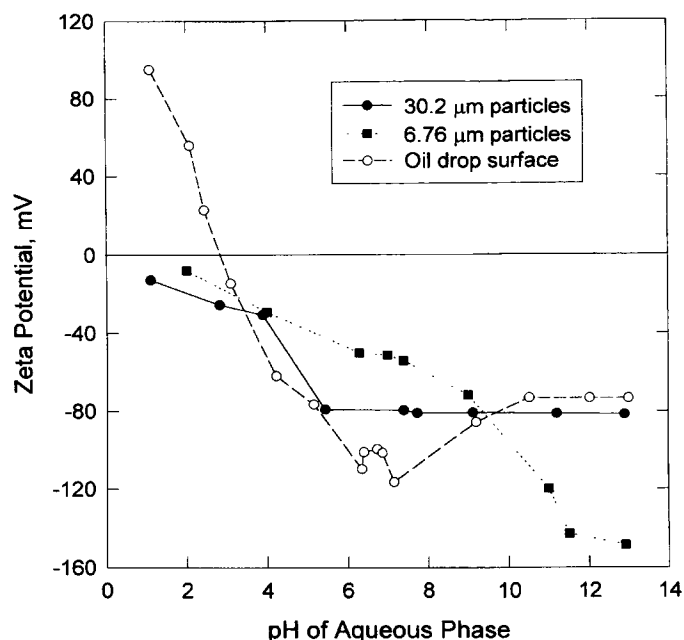
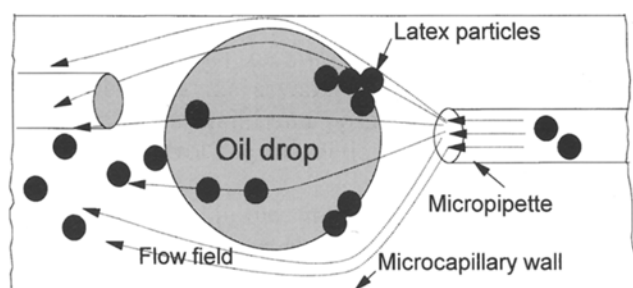


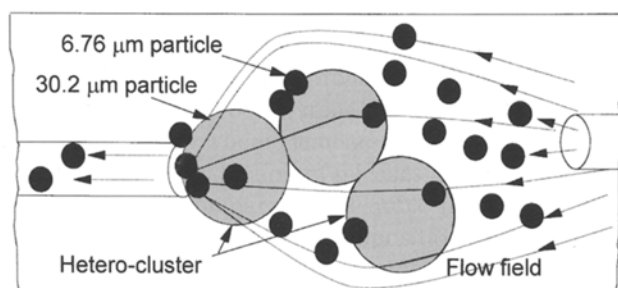
Fig. 1 Variation of zeta potentials with solution pH

and Cl^-) at the given pH of the dispersion was ascertained, the zeta potentials were calculated from the electrophoretic mobility using the modified Booth equation [11, 21]. The electrophoretic mobilities and zeta potentials of the small particles were measured previously [15] using the Doppler–electrophoretic–laserlight–scattering–analyser (DELSA) model 440 supplied by Coulter Electronics Inc. Hialeah, FL, USA. Variation of zeta potentials with solution pH for the two types of polystyrene particles is shown in Fig. 1. It can be seen that the negative zeta potentials of the 6.76 μm particles are significantly higher than those for the 30.2 μm particles for pHs greater than 10. The variation of zeta potential with solution pH for the oil drop surface was also determined earlier [11] and the data are also shown in Fig. 1.

The video-microscopy set up is described elsewhere [11]. The central portion of the glass microcapillary where the interactions were conducted is shown in Fig. 2. The glass microcapillary (i.d., 100–160 μm) was made by “pulling” a commercially available glass pipette (7000 μm i.d.) in the center, whereas the glass micropipette was made by “pulling” the glass pipette from one end. Aqueous solution containing the particles was drawn into the microcapillary by means of a syringe after repeatedly rinsing its inside surface with the solution. Two micropipettes were introduced, one from each end, into the microcapillary. Oil drops were produced in situ at the tip of one of the micropipettes and released into the aqueous medium inside the microcapillary. The other micropipette was used



(a)



(b)

Fig. 2 Procedure for: (a) Conducting interactions of particles with the oil drop. (b) Forming a hetero-cluster of latex particles

to move the suspended particles and make them interact with the surface of the oil drop. The two micropipettes also helped in keeping the drop(s)/particle(s) in the viewing field of the microscope.

Interaction and aggregation among *n*-hexadecane oil drops and the polystyrene latex particles of two different sizes was studied visually at eight different pH conditions

of the aqueous phase in the following three cases: (i) polystyrene latex particles with one oil drop (hetero-aggregation); (ii) two different types of polystyrene latex particles (hetero-aggregation); and (iii) same type of polystyrene latex particles (homo- or selective aggregation). The visual observations vis-a-vis the theoretical DLVO predictions for each case are discussed in the following section.

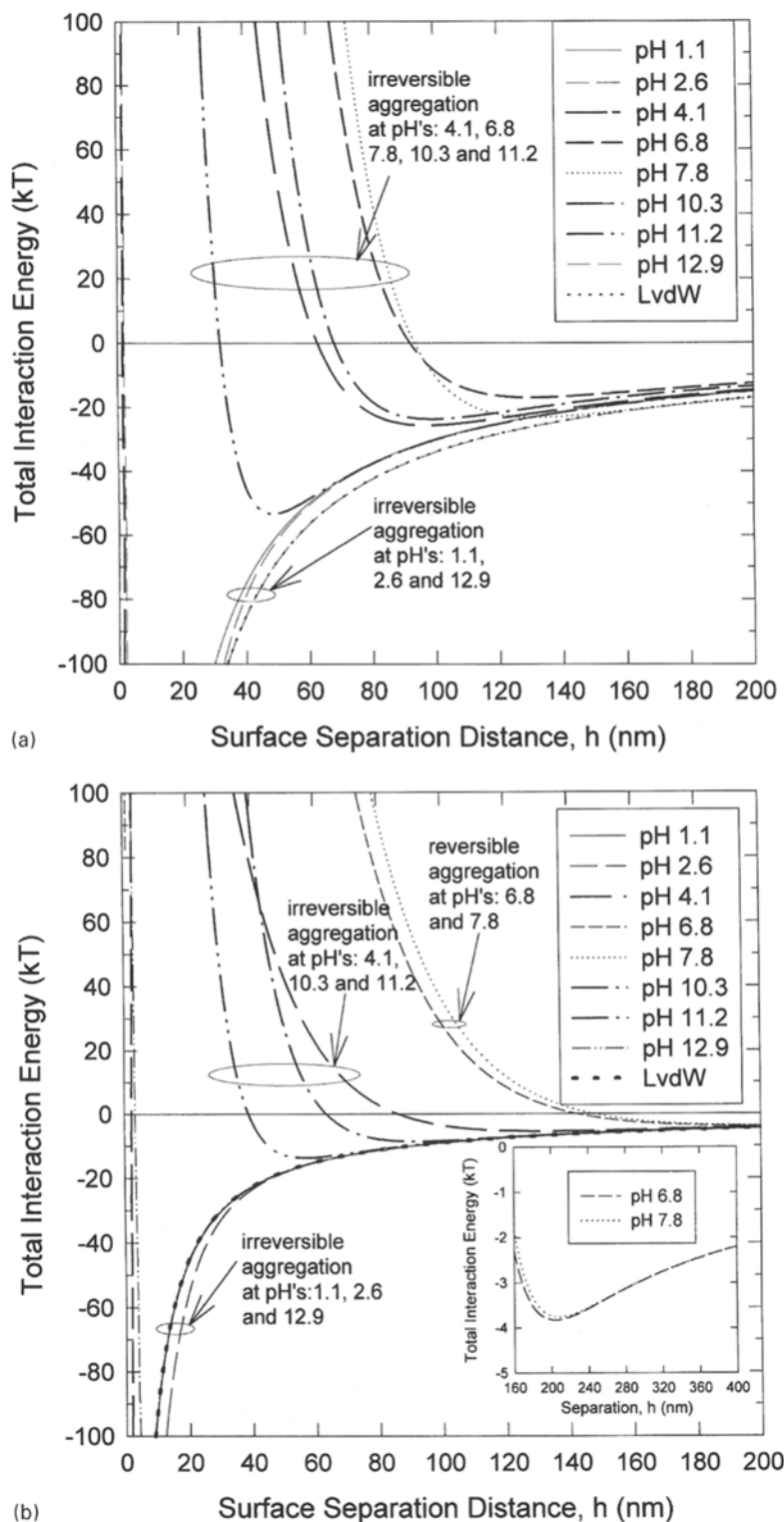
Results and discussion

Theoretical predictions of the outcome of interactions between drops and particles are examined based on the DLVO diagrams where V_T , the total interaction free energy, is normalized by kT and is plotted against the surface-to-surface separation distance, h . The parameters required to compute the total interaction energies from Eqs. (1)–(3) are the boundary electrostatic potentials, the radii of the drops and the particles, and the Debye parameter, κ . Values for these parameters are given in Table 1. For each pH shown in Table 1, the zeta potentials were obtained by interpolation from Fig. 1. Starting around neutral pH, it may be seen in Table 1 that, as the pH increases or decreases, the ionic strength of the aqueous phase always increases corresponding to a decrease in the Debye length, κ^{-1} . The reduction in Debye length means that a major portion of the EDL repulsion is confined to distances of separation smaller than κ^{-1} , and that at such conditions the interfaces are able to approach each other much closer. However, changes in pH may at the same time comport surface potential increases which augment EDL repulsion. These inter-dependencies of ionic strength and surface potential on the outcome of interactions is best explained by the DLVO interaction free energy diagrams. In the DLVO diagrams, the sign and magnitude of the

Table 1 Parameters used in the determination of the DLVO interaction free energies

pH	Interactions of oil drop and 30.2 μm latex particles		Interactions of oil drop and 6.76 μm latex particles		Interactions of 6.76 and 30.2 μm particles κ^{-1} [nm]	Interactions of two 30.2 μm particles κ^{-1} [nm]	Interactions of two 6.76 μm particles κ^{-1} [nm]	Zeta potential of drop surface ζ [mV]	Zeta potential of 6.76 μm particles ζ [mV]	Zeta potential of 30.2 μm particles ζ [mV]
	drop dia. [μm]	κ^{-1} [nm]	drop dia. [μm]	κ^{-1} [nm]						
1.1	64.00	1.522	84.00	1.526	1.078	1.522	1.526	+ 95.00	+ 1.56	– 12.88
2.6	66.00	7.488	78.00	8.080	5.492	7.488	8.080	+ 14.27	– 14.36	– 24.00
4.1	60.00	14.523	42.00	19.415	11.980	14.523	19.415	– 56.77	– 30.12	– 36.98
6.8	40.00	15.222	60.00	23.577	12.790	15.222	23.577	– 100.53	– 50.77	– 79.25
7.8	110.00	15.212	60.00	23.540	12.790	15.212	23.540	– 106.53	– 58.37	– 80.90
10.3	47.00	12.440	70.00	11.257	11.003	12.440	11.257	– 75.14	– 102.94	– 80.95
11.2	66.00	6.840	66.00	7.282	6.569	6.840	7.282	– 73.10	– 128.96	– 81.17
12.9	102.00	1.079	75.00	1.080	1.078	1.079	1.080	– 73.21	– 148.60	– 81.56

Fig. 3 DLVO curves for interaction between the surfaces of oil drop and:
(a) 30.2 μm latex particle, and
(b) 6.76 μm latex particle



slope of the total interaction free energy curve gives the force of attraction (positive slope) or repulsion (negative slope). Also, the position of the secondary minimum indi-

cates how close the surfaces can approach each other before they experience strong repulsion due to the electrical double layer.

Hetero-aggregation of particles with an oil drop

Interactions between an oil drop and polystyrene latex particles were conducted as schematically described in Fig. 2a. The flow field was repeatedly used (i) to facilitate the motion of the particles in the bulk liquid so as to bring them into contact with the drop, and (ii) to cause detachment of those particles already adhering to the drop's surface. Experiments were conducted with each of the two types of polystyrene particles separately at eight different pHs. Significant differences were observed in the nature of attachment of the two particles onto the oil drop as the pH was varied from 1.1 to 12.9. The DLVO curves for interaction between an oil drop and a latex particle at the various pHs are shown in Figs. 3a and 3b, for the 30.2 and 6.76 μm particles, respectively. The attractive London-van der Waals free energy, not a strong function of pH, is independently shown by the curve designated LvdW, which notably almost coincides with the total interaction free energy curves at pHs 1.1, 2.6 and 12.9.

Visual observations showed irreversible attachment of both particles onto the oil drop's surface in almost all cases. For both small and large particles, the attachment was spontaneous at pHs 1.1, 2.6 and 12.9. Video snapshots of the attachment are shown in Figs. 4a and 4b. At other pHs, collection of particles on the drop surface was not spontaneous and it took some time before the particles became irreversibly attached. Here, irreversible aggregation means that the particles could not be detached from the drop's surface even after repeated attempts to dislodge them using the flow field. Only in two cases the attachment was reversible viz. pHs 6.8 and 7.8 for the small latex particles. Figure 4c shows the detachment of 6.76 μm particles from the drop surface. These observations may be explained with the DLVO theory as follows.

For the 30.2 μm particles as well as the 6.76 μm particles, Figs. 3a and 3b show that the total interaction free energy, at the three pHs (1.1, 2.6 and 12.9) where spontaneous attachment was seen, is continuously attractive from distances of separation greater than 200 nm down to very short separation distances. Furthermore, for pHs 1.1, 2.6 and 12.9 the secondary minimum's depth is significantly larger than $100kT$. Therefore the spontaneous attachment may be explained as a result of this attractive interaction. There are two possible ways for particles to attach themselves onto the oil drop: (i) particle entrapment in the secondary minimum and (ii) rupture of the aqueous film between the drop and the interacting particle, in which instance the particle is, at least partially, wetted by the oil. In the case of secondary minimum (weak) entrapment, the particles would be expected to glide freely on the drop's surface and to detach from it when subjected to sufficient hydrodynamic force. Since this behavior was not exhibited

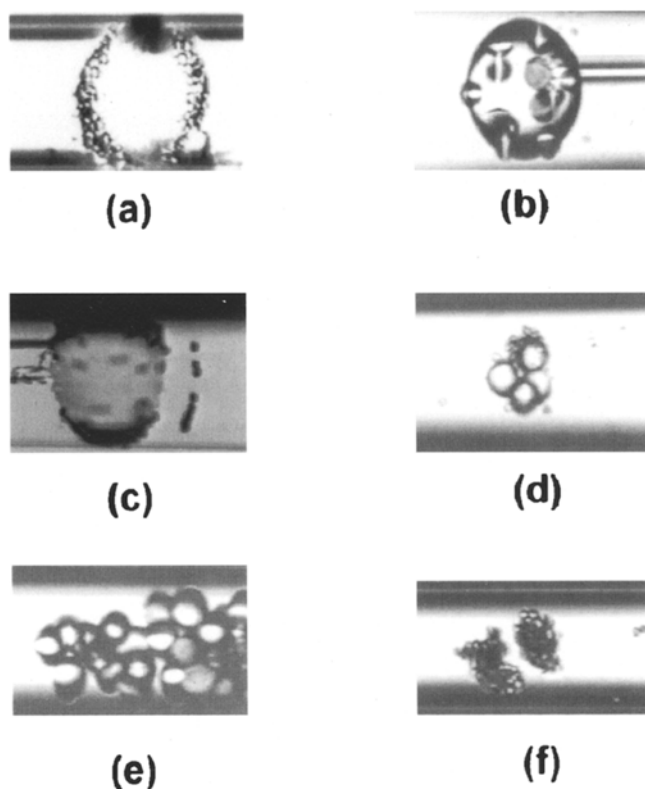


Fig. 4 (a) Irreversibly attached 6.76 μm latex particles on the oil drop surface at pH 1.1, (b) irreversibly attached 30.2 μm latex particles on the oil drop surface at pH 12.9, (c) detachment of gliding 6.76 μm latex particles from the drop surface at pH 6.8, (d) hetero-aggregation of 6.76 μm and 30.2 μm latex particles at pH 2.6, (e) selective-aggregation of 30.2 μm latex particles at pH 7.8, and (f) selective-aggregation of 6.76 μm latex particles at pH 2.6

at the said pHs, it may be concluded that the attachment mechanism involved film rupture.

At pHs 4.1, 10.3 and 11.2, the DLVO curves show the secondary minimum to be between 50–125 nm and the minimum's depth to be in the range ~ 15 – $55kT$. Even though the well is much shallower than at pHs 1.1, 2.6 and 12.9, irreversible aggregation was observed indicating partial wetting. Recorded video images showed that the particles with the drop together translated and rotated as one entity in the aqueous medium.

Particle gliding and reversible aggregation were observed at pHs 6.8 and 7.8 only in the case of small latex particles, suggesting that the aqueous film between the particles and the oil drop is stable. At both pHs, it took some time to collect enough number of 6.76 μm particles on the surface of the oil drop, in contrast to the 30.2 μm particles which collected readily. Such an outcome for the 30.2 μm particles is expected since the LvdW attraction increasingly dominates the total interaction as particle size increases. This can be readily seen by comparing the

LvdW curves in Figs. 3a and 3b, as well as the total interaction curves for the said pHs. The inset in Fig. 3b shows a secondary minimum at 200 nm for pHs 6.8 and 7.8

and the depth of the secondary well to be only $3.8kT$. Repulsive DLVO forces rise exponentially for lower separations. It is suggested that the repulsive forces, which are

Fig. 5 DLVO curves for interaction between the surfaces of: (a) 6.76 and 30.2 μm latex particles, (b) two 30.2 μm latex particles, and (c) two 6.76 μm latex particles

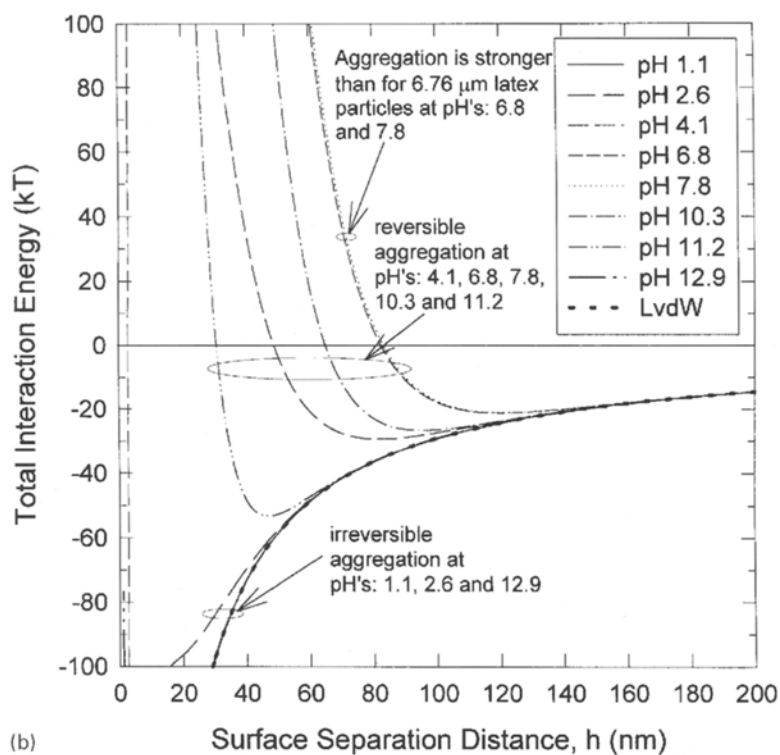
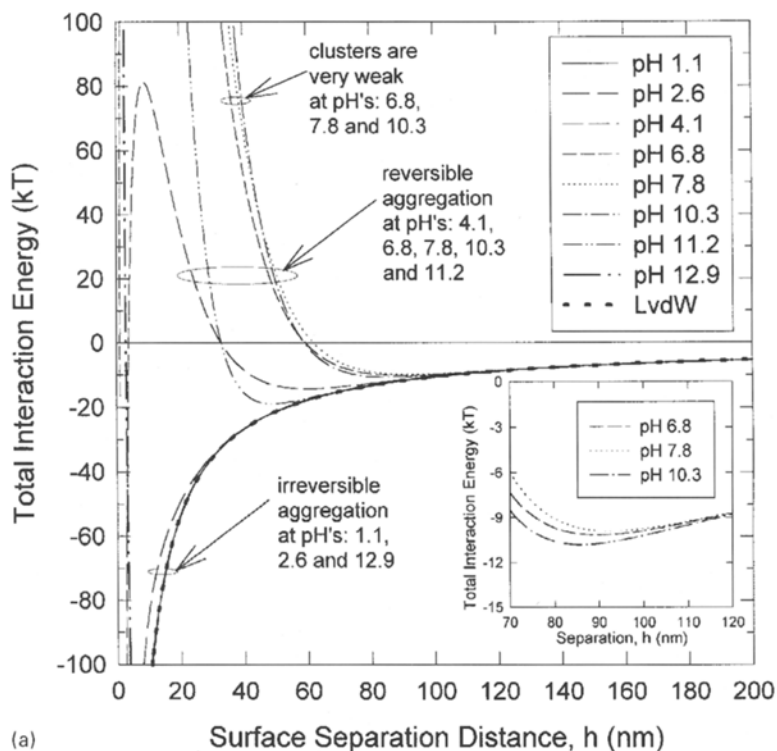
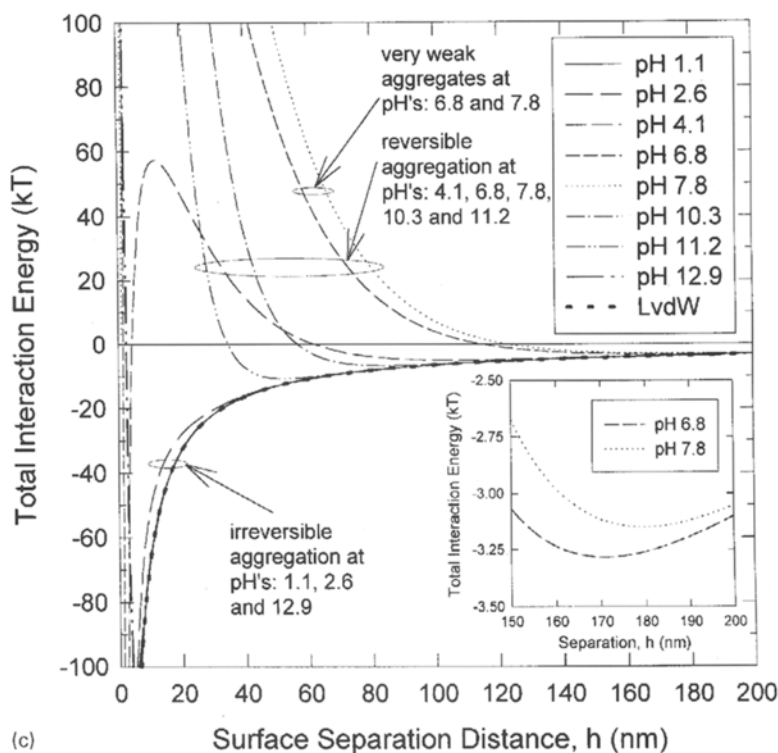


Fig. 5 Continued



in effect even at large separation distances, decelerate the small particle and the reduced hydrodynamic force is not effective in overcoming the repulsion so as to further reduce the thickness of the film to some critical thickness for rupture. It is therefore believed that in the experiments on drop-particle interactions, secondary minimum attachment and reversible aggregation occurred exclusively for the small particles and at pHs 6.8 and 7.8.

Hetero-aggregation of latex particles

Interactions among the two different types of latex particles (6.76 and 30.2 μm) were conducted as shown in Fig. 2b. The aqueous solution containing both types of particles thoroughly dispersed in it was first introduced into the microcapillary. A micropipette was then inserted into the microcapillary from one of its ends and the aqueous solution was withdrawn, thus facilitating the motion of particles in the solution and their collection at the tip of the micropipette. In this way, a hetero-aggregate containing both large and small particles could be formed at the micropipette tip. To release the cluster into the bulk solution the flow direction was reversed. By repeatedly performing this operation, it was possible to visualize whether the cluster broke-up or remained intact. Visual observa-

tions showed that clusters could be formed at all pHs. Aggregation was irreversible at pH 1.1, 2.6 and 12.9 and reversible at all the other pHs. Clusters were most reversible and easily broken at pHs of 6.8 and 7.8. A video snapshot of a hetero-cluster is shown in Fig. 4d.

The DLVO interaction free energy curves are shown in Fig. 5a. At the pHs of 1.1, 2.6 and 12.9, the curves show continuous attraction between the surfaces of the dissimilar particles from separations starting at several hundred nm until the secondary minimum. The secondary minimum in these three cases occurs below 10 nm and the significant well depth (greater than $100kT$) indicates that the surfaces of the two particles attract each other strongly. Therefore, once two particles are in close proximity there is spontaneous attraction between the surfaces which results in the formation of a strong hetero-cluster. At pHs of 6.8, 7.8 and 10.3, the secondary minimum occurs at a separation distance of about 85 nm, is relatively shallow (well depth $\sim 10kT$) and there is an exponential increase in repulsion for lower separations. Thus, at these pHs the particles are weakly attracted to each other and a flow field can easily detach the weak aggregate. Observations also showed that the reversible hetero-aggregates of latex particles broke up upon repeated movement inside the microcapillary and smaller and stronger homo-aggregates were formed.

Selective aggregation of latex particles

The procedure for forming homo-aggregates was essentially the same as described in Fig. 2b except that the aqueous solution introduced into the microcapillary now contained only one type of particles. Visual observations showed strong aggregation and cluster formation at pHs 1.1, 2.6 and 12.9 for both types of particles. Video snapshots of homo-aggregates of the large and small latex particles are shown in Figs. 4e and 4f. At these pHs, clusters could not be broken into individual particles by slow repeated movement inside the microcapillary, though it was possible to break a large cluster into smaller clusters. The DLVO curves for the 30.2 and 6.76 μm particles are shown in Figs. 5b and 5c, respectively. In both figures, the curves show strong attraction between the particle surfaces at the pHs of 1.2, 2.6 and 12.9, in agreement with the visual observa-

tions of strong aggregation at these pHs. At the pHs of 6.8 and 7.8, Fig. 5b shows that the secondary minimum for the 30.2 μm particles occurs at ~ 120 nm, the secondary well is moderately deep ($\sim 20kT$) and there is a strong attractive interaction between the particle surfaces until the secondary minimum. For the 6.76 μm particles (Fig. 5c) at the same pHs, the secondary minimum occurs between separations of 170 and 180 nm, the secondary well (inset) is very shallow at a depth of only $\sim 3.2kT$ indicating weak attraction between the small particles. Both of these theoretical results conform with the visual observations of strong clustering in the case of larger particles and very weak clustering for smaller particles.

Acknowledgments Financial support from the National Science Foundation (Grant OSR-9108765) and through the Tulane/Xavier DoD Center for Bioenvironmental Research (CBR) is gratefully acknowledged.

References

1. Somasundaran P (ed) (1980) In: Fine Particles Processing. AIME, New York
2. Hunter RJ (1986) Foundations of Colloid Science, Vols. I and II. Oxford University Press, New York
3. Pugh RJ, Kitchener JA (1971) *J Colloid Interface Sci* 35:656
4. Bleier A (1976) Stability of Mixed Colloidal Dispersions. PhD Thesis, Clarkson College of Technology, Potsdam, New York
5. Qun Wang (1991) *J Colloid Interface Sci* 145:305
6. Hogg R, Healy TW, Fuerstenau DW (1966) *Trans Faraday Soc* 62:1638
7. Thibodeaux LJ (1996) *Environmental Chemodynamics*, 2nd ed. Wiley-Interscience, New York
8. Derjaguin BV (1954) *Discuss Faraday Soc* 18:85
9. Marmur A (1979) *J Colloid Interface Sci* 72:41
10. Yato A, Papadopoulos KD (1985) *Colloids and Surfaces* 16:55
11. Deshiikan RS, Papadopoulos KD (1995) *J Colloid Interface Sci* 171:303
12. Deshiikan RS, Papadopoulos KD (1995) *J Colloid Interface Sci* 171:313
13. Liu Z, Papadopoulos KD (1995) *Appl Environ Microbiol* 61:3567
14. Liu Z, Papadopoulos KD (1996) *Biotechnol Bioeng* 51:120
15. Kuo C-C, Papadopoulos KD (1996) *Environ Sci Technol* 30:1176
16. Hou W, Papadopoulos KD (1996) *Chem Eng Sci* 51:5043
17. Chen JD, Hahn PS, Slattery JC (1984) *AIChE J* 30:622
18. Derjaguin BV, Landau LD (1941) *Acta Physico-chim URSS* 14:633
19. Verwey EJW, Overbeek JThG (1948) *Theory of the Stability of Lyophobic Colloids* Elsevier, Amsterdam
20. Sader JE, Carnie SL, Chan DYC (1995) *J Colloid Interface Sci* 171:46
21. Hunter RJ (1981) *Zeta Potential in Colloid Science*. Academic Press, New York